

DESI-Like Hubble Expansion From Staged Symmetry Breaking

Zachary J. Hoelscher, Thomas W. Kephart, and Robert J. Scherrer

*Department of Physics and Astronomy, Vanderbilt University, Nashville, TN 37235, USA**

Kelly Holley-Bockelmann

Department of Physics and Astronomy, Vanderbilt University, Nashville, TN 37235, USA and*

Department of Life and Physical Sciences,

Fisk University, Nashville, TN 37208, USA

(Dated: December 8, 2025)

The Dark Energy Spectroscopic Instrument (DESI) second data release shows a moderate preference for dark energy with a time-varying equation of state parameter, suggesting that the standard Λ CDM model may need to be revised. In particular, DESI favors dark energy whose equation of state parameter can drop below -1 , violating the null energy condition. Chen and Loeb have recently suggested that this violation may be avoided if a subcomponent of the dark matter possesses a time-dependent equation of state. In this work, we present a realization of that idea which can be regarded as a more natural effective field theory. We show that such a construction not only yields dark matter with a time-varying equation of state parameter, but also naturally produces a self-interacting dark matter candidate with a velocity-dependent cross section as a consequence of gauge invariance. The second feature is relevant for addressing tensions between Λ CDM and observations of small-scale structure, particularly the diversity of galactic rotation curves.

I. INTRODUCTION

Since the accelerating expansion of the Universe was first discovered in 1998 [1, 2], the mysteries of dark energy have intrigued the scientific community. While the simplest explanation for this acceleration is a cosmological constant, others have suggested that dark energy could be explained by the addition of a new scalar field [3–5], which could allow for dynamical dark energy [6]. The recent Dark Energy Spectroscopic Instrument (DESI) results show up to a 4.2σ preference for a dynamical equation of state parameter for dark energy, perhaps motivating alternatives beyond the standard Λ CDM paradigm [7–9], such as modifications to cold dark matter [10–16]. Strikingly, some have even found a 5σ preference [17].

The DESI results also prefer a model of dark energy that exhibits phantom behavior, meaning an equation of state parameter that drops below -1 [9]. Such behavior seemingly violates the null energy condition, $T_{\mu\nu}k^\mu k^\nu \geq 0$ [18].

In an effort to avoid this, recent work proposes that the DESI results could instead be explained by a combination of a cosmological constant and a subcomponent of dark matter with a time-varying equation of state parameter [19]. In this work, they assume that the subcomponent has a density parameter that is around one-fifth of the density parameter for the other matter content. They also assume that its equation of state parameter exhibits step-like changes between constant values over the range -0.5 to 0.5 , and they examine a few scenarios for $w(z)$.

In particular, Chen and Loeb [19] adopt the following potential $V(\phi)$ to motivate this, where $\phi_1 \gg \phi_2 > 0$:

$$V(\phi) \propto f(\phi)^6 / (\phi_1^4 + f(\phi)^4), \quad (1)$$

and

$$f(\phi) = \left(\phi_2^{16/3} + |\phi|^{16/3} \right)^{1/6} |\phi|^{1/9}. \quad (2)$$

Unfortunately, this potential is non-renormalizable and lacks a clear, natural UV completion (a form of the theory that is valid at high energy scales), which is needed

* zachary.j.hoelscher@vanderbilt.edu

for a fully consistent theory. They emphasize, however, that this is but one possible example. A following paper adopts a different model, though this is again non-renormalizable, so one again has divergences that cannot be removed using a finite number of counterterms [20].

In this work, we build on the idea by providing an example of a more natural effective field theory that can exhibit similar behavior. While it may at first seem that one could construct any arbitrary variation of the equation of state parameter by reverse-engineering a potential like the one given above, this is not the case. For a model to be physically sound as a quantum field theory, it needs a UV completion. It is desirable for a theory to emerge from a natural, renormalizable Lagrangian. One can treat some non-renormalizable theories as effective field theories, though without a UV completion, such a model is potentially unphysical. We are unable to produce a field theory that exhibits the desired behavior while being fully renormalizable, though in our case, all interactions are renormalizable, except one.

This model is additionally interesting for producing a potential self-interacting dark matter (SIDM) candidate as a by-product of gauge invariance. SIDM has been proposed to resolve tensions between Λ CDM and observations of small-scale structure, such as the diversity of rotation curves in dwarf galaxies [21–23]. Λ CDM without baryonic physics predicts cuspy NFW density profiles [24–26], yet some dwarf galaxies are observed to have cored profiles [21, 27–30]. Cores can be produced via baryonic feedback [31–45], however some observed dwarf galaxies have too few stars to easily explain their density profiles through such means [46]. SIDM alleviates these tensions by flattening the central density profile of the dark matter halo, which is achieved through non-gravitational interactions between particles [21].

Our SIDM candidate consists of a heavy vector field interacting through a scalar mediator. Vectors interacting through a scalar have been considered before as an SIDM candidate [47], though our case is interesting because the SIDM arises naturally as a by-product of constructing

a consistent theory, rather than something that was arbitrarily postulated. We find that the interaction cross section is velocity-dependent, which is desirable to allow SIDM to produce cored halos at the galaxy scale while also satisfying constraints from galaxy clusters [48–50].

II. DISCUSSION OF POSSIBLE MODELS

We wish to produce a dark matter model whose equation of state parameter shifts between four values: w_1, w_2, w_3 , and w_4 . To do this, we consider a decay cascade of the form $A \rightarrow B \rightarrow C \rightarrow D$. This cascade concept is similar to the dynamical dark matter considered by Dienes [51–53], though our work contains a finite number of stages, rather than an infinite number, and is motivated by DESI observations. In addition to our fiducial model, we briefly discuss alternatives and outline the problems with them.

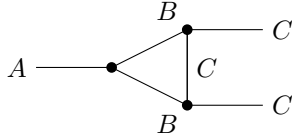
A. Four Real Scalar Fields

The simplest construction one might try would be a decay cascade involving four real scalar fields (A, B, C, and D), similar to that shown below:

$$\mathcal{L} \supset \sum_{\Phi \in \{A, B, C, D\}} \left[\frac{1}{2} \partial^\mu \Phi \partial_\mu \Phi - \frac{1}{2} m_\Phi^2 \Phi^2 - \lambda_\Phi \Phi^4 \right] - g_{AB} AB^2 - g_{BC} BC^2 - g_{CD} CD^2, \quad (3)$$

where this model permits a decay cascade $A \rightarrow B \rightarrow C \rightarrow D$ via tree-level processes such as $A \rightarrow 2B$. (Note that a “tree-level” process is the lowest-order perturbative approximation for a decay or scattering process.) This model is arguably unnatural, though, as there is no symmetry-motivated reason to exclude the couplings $g_{AC} AC^2$, $g_{AD} AD^2$, and $g_{BD} BD^2$ when we have already broken the \mathbb{Z}_2 symmetry of the theory (invariance of the action under a sign flip of a field) by including the terms $g_{AB} AB^2$, $g_{BC} BC^2$, and $g_{CD} CD^2$. Terms like $g_{AC} AC^2$

would allow the decay chain to skip stages, if included. In any case, unwanted decay processes will still occur at one-loop via diagrams like the one shown below, which yields $A \rightarrow 2C$. Such diagrams would allow the decay chain to skip stages, and are still undesirable, although they are suppressed by extra factors of coupling constants.



Such a model also results in a suppressed effect on the Hubble parameter $H(z)$ because it does not enforce a rapid shift of energy density from one field to another. In effect, while A is decaying to B , B is decaying to C , and C to D , so at any given time, there is a mixture of the four fields, rather than a clean shift of the energy density from one field to another.

B. Four Complex Scalar Fields With Global Symmetry

We can ensure a clean shift of energy density from one field to another (so the effect on $H(z)$ is not suppressed) by using complex scalars with appropriate charges. One could spontaneously break a global $U(1) \times U(1) \times U(1)$ symmetry to sequentially turn on two-body decays of the form $A \rightarrow B^\dagger B$. Sequentially turning on decays in this way helps to ensure a clean shift of energy density between fields.

Such a model still has an issue, however. Global symmetries are believed to be inconsistent once embedded in a full theory of quantum gravity [54]. Even without appealing to quantum gravity consistency, one can argue that gauge symmetries are natural. Global symmetries expected to be only approximate at best, with gauge symmetries taking primacy [55]. This conjecture can be motivated by the AdS/CFT correspondence [54], which can be regarded as a toy model for quantum gravity where anti-de Sitter space (AdS) is dual to a conformal field theory (CFT). Our Universe is

not anti-de Sitter, as the cosmological constant is believed to be positive, rather than negative, though the arguments used for AdS/CFT could perhaps be generalized to flat-space holography, which would describe a Universe with a vanishing cosmological constant, and would be a more useful approximate model for our Universe.

When considering continuous global symmetries, the case that they are inconsistent can also be motivated by the black hole information paradox, in which case the argument can be generalized beyond the AdS/CFT correspondence [56]. One can loosely motivate this by arguing that continuous global symmetries imply conserved charges that are destroyed by black hole evaporation, therefore continuous global symmetries should not exist in nature, as we expect black hole evaporation to be unitary. This argument is more restrictive than the AdS/CFT result, as it applies to continuous global symmetries, such as $U(1)$, but not global symmetries in general.

C. Our Fiducial Model

We have four complex scalar fields A , B , C , and D , with four dark Higgs fields H_1 , H_2 , H_3 , and H_4 . We use complex scalar fields because charge assignments allow us to enforce a decay chain. One might initially suspect that a scalar field will not clump as dark matter because the kinetic terms could imply a sound speed of c , though there is no such problem [19], which we discuss further in the Appendix.

Since the theory has a $U(1) \times U(1) \times U(1) \times U(1)$ gauge group, we must introduce four gauge bosons to allow for gauge invariance: α_μ , β_μ , γ_μ , and δ_μ , where we define the Faraday tensors as $\Psi_{\mu\nu} = \partial_\mu \Psi_\nu - \partial_\nu \Psi_\mu$, and the covariant derivative as $\mathcal{D}_\mu \equiv \partial_\mu - i(g_1 q_1 \alpha_\mu + g_2 q_2 \beta_\mu + g_3 q_3 \gamma_\mu + g_4 q_4 \delta_\mu)$. We note that a similar gauge group, $U(1) \times U(1) \times U(1)$, can arise in string theory [57]. We also note that anomalies will not be present, as the model does not incorporate fermions [58]. We can express \mathcal{L} as follows. For simplicity, we assume any mixed quartics of the form $(H_1^\dagger H_1)(H_2^\dagger H_2)$ have small coupling constants, and can be neglected.

$$\begin{aligned}
\mathcal{L} \supset & \mathcal{D}^\mu A^\dagger \mathcal{D}_\mu A - m_A^2 A^\dagger A + \mathcal{D}^\mu B^\dagger \mathcal{D}_\mu B - m_B^2 B^\dagger B \\
& + \mathcal{D}^\mu C^\dagger \mathcal{D}_\mu C - m_C^2 C^\dagger C + \mathcal{D}^\mu D^\dagger \mathcal{D}_\mu D - m_D^2 D^\dagger D - \kappa H_1^\dagger H_1 \sqrt{C^\dagger C} \\
& - \left(g_{AB} H_2^\dagger A B^\dagger B + g_{BC} H_3^\dagger B C^\dagger C + g_{CD} H_4^\dagger C D^\dagger D + \text{h.c.} \right) \\
& - \sum_{\Psi_\mu \in \{\alpha_\mu, \beta_\mu, \gamma_\mu, \delta_\mu\}} \left[\frac{1}{4} \Psi_{\mu\nu} \Psi^{\mu\nu} \right] + \sum_{i=1}^4 \left[\mathcal{D}^\mu H_i^\dagger \mathcal{D}_\mu H_i + m_{H_i}^2 H_i^\dagger H_i - \lambda_{H_i} (H_i^\dagger H_i)^2 \right]
\end{aligned} \tag{4}$$

Note that we use “h.c.” to denote the hermitian conjugate. The action is invariant under local transformations of the form $\Phi \rightarrow e^{iq\alpha(x)}\Phi$, with q denoting the charge, where we indicate the charge assignments in the table below. If we had a global symmetry, we would instead have transformations of the form $\Phi \rightarrow e^{iq\alpha}\Phi$, and would not require gauge bosons, such as α_μ .

Field	$U_1(1)$	$U_2(1)$	$U_3(1)$	$U_4(1)$
A	0	1	0	0
B	0	0	1	0
C	0	0	0	1
D	0	0	0	1
H_1	1	0	0	0
H_2	0	1	0	0
H_3	0	0	1	0
H_4	0	0	0	1

TABLE I. Charge assignments for our fields under $U_1(1) \times U_2(1) \times U_3(1) \times U_4(1)$.

Each time a $U(1)$ is spontaneously broken, a dark Higgs field gains a non-zero vacuum expectation value. This then sequentially turns on the terms of the form $\sqrt{C^\dagger C}$, $AB^\dagger B$, $BC^\dagger C$, and $CD^\dagger D$, where charge conservation forbids both two and three-body decays until the relevant $U(1)$ symmetries are broken.

The terms $AB^\dagger B$, $BC^\dagger C$, and $CD^\dagger D$ enable decays from one field to another, whereas the square root term allows C to have a negative equation of state parameter. The equation below yields the equation of state parameter $w(R)$ for a complex scalar field, which can be written in terms of its magnitude, R , and phase factor, ϕ , giving $Re^{i\phi}$ [59].

$$w(R) \approx \frac{RV'(R) - 2V(R)}{RV'(R) + 2V(R)} \tag{5}$$

Here, the equation of state parameter is $w = 0$ for a quadratic potential and $w = -1/3$ for a potential that is linear in the magnitude, R , where the linear term dominates. One can alternatively obtain $0 < w < 1/3$ from semi-relativistic decay products. This is more natural than $w = 1/3$ from a strongly-coupled quartic interaction that dominates the potential. If the field C is oscillating in a potential that has both a term linear in the magnitude (our square root term $H_1^\dagger H_1 \sqrt{C^\dagger C}$) and a quadratic mass term, but where the former term dominates, one obtains $w \approx -1/3$. Since H_1 obtains a VEV (vacuum expectation value) at early times, this square root term can naturally dominate after $U_1(1)$ is broken. We use this rather than a renormalizable term like $H_1^\dagger C$ because $H_1^\dagger C$ exhibits phase-dependence in addition to dependence on the magnitude, R , which complicates the dynamics. This square root term for a complex scalar is analogous to a potential $|\phi|$ for a real scalar ϕ , as R is strictly positive. Note that the square root term for C turns on before any decays begin, as the associated $U(1)$ is broken first, though this term has no effect on the system until C is produced from decays later on.

One could alternatively achieve a transiently negative equation of state parameter for C by giving it a Higgs-like potential, which would be simpler and more natural. The problem is that in order to get a lasting $w_C < 0$, the field would have to slow-roll on the potential, which would require such a small mass that the field would

be quintessence-like, rather than a dark matter field. We consider the necessity of a transiently negative equation of state parameter to be one of the greatest difficulties in producing a natural, renormalizable realization. One could also consider cosmic strings produced from breaking a $U(1)$, though these may not produce a significant enough effect.

D. Self-Interacting Dark Matter Candidate From Our Fiducial Model

After the first $U(1)$ is broken, yielding a dark Higgs with a mass of $\mathcal{O}(\text{MeV})$, the term $\mathcal{D}^\mu H_1^\dagger \mathcal{D}_\mu H_1$ produces an interaction of the form $gh\alpha_\mu\alpha^\mu$, which permits an $\alpha\alpha \rightarrow \alpha\alpha$ scattering processes via a scalar mediator, as shown below. Note that h is the radial mode of the dark Higgs, after symmetry breaking gives it a mass. For $\alpha \sim \text{GeV}$ and $h \sim \text{MeV}$, our fiducial model produces a natural SIDM candidate, one that could conceivably address some of the issues with CDM if α comprises the bulk of the dark matter. We show the t and u -channel Feynman diagrams in Figure 1.

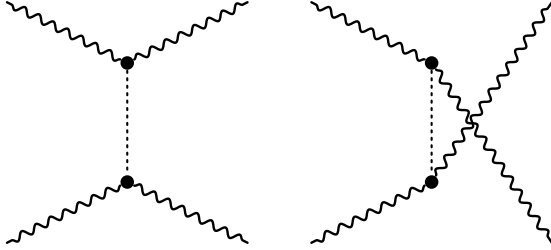


FIG. 1. We show Feynman diagrams for tree-level $\alpha\alpha \rightarrow \alpha\alpha$ scattering via a scalar mediator h . The t -channel diagram is shown on the left and the u -channel diagram on the right.

III. METHODS

A. $H(z)$ From Our Fiducial Model

We numerically integrate the following system of coupled differential equations to calculate the evolution of the Hubble parameter with cosmic time. We assume that dark matter is 85% of the total matter density, and that the dark field A comprises 20% of the total dark

matter at recombination. Note that $\Theta(t - t_i)$ is a step function that becomes nonzero after $U_i(1)$ is broken.

We have equation of state parameters $w_A = 0$, $w_B = \frac{1}{12}$, $w_C = -\frac{1}{3}$, and $w_D = \frac{1}{12}$, where B and D are warm dark matter. We use $\Gamma_A = \Gamma_B = \Gamma_C = 10^{-15} \text{ sec}^{-1}$. (See the Appendix for the equation that expresses the decay rate in terms of the masses and coupling constants.) In the equations below, ρ_A , ρ_B , ρ_C , and ρ_D are the densities of the complex scalars in the cascade, whereas ρ_O is the density of the other matter (baryons+other dark matter), ρ_r is the radiation density, and ρ_Λ is the dark energy density. In the equations below, t_2 , t_3 , and t_4 correspond to redshifts of 3, 1.5, and 0.6. We note that the square root term for C (which gives it $w < 0$) turns on at early times when α_μ gains a mass, though this term does not have an effect until C is produced from decays of B . We neglect any energy transfer to the massive radial modes of the dark Higgs fields via three-body decays after the relevant $U(1)$ symmetries are broken; a more detailed analysis could consider this.

$$\dot{\rho}_A + 3H(1+w_A)\rho_A = -\Theta(t-t_2)\Gamma_A\rho_A \quad (6a)$$

$$\begin{aligned} \dot{\rho}_B + 3H(1+w_B)\rho_B &= \Theta(t-t_2)\Gamma_A\rho_A \\ &\quad - \Theta(t-t_3)\Gamma_B\rho_B \end{aligned} \quad (6b)$$

$$\begin{aligned} \dot{\rho}_C + 3H(1+w_C)\rho_C &= \Theta(t-t_3)\Gamma_B\rho_B \\ &\quad - \Theta(t-t_4)\Gamma_C\rho_C \end{aligned} \quad (6c)$$

$$\dot{\rho}_D + 3H(1+w_D)\rho_D = \Theta(t-t_4)\Gamma_C\rho_C \quad (6d)$$

$$H^2 = \frac{8\pi G}{3}(\rho_A + \rho_B + \rho_C + \rho_D + \rho_O + \rho_r + \rho_\Lambda) \quad (7)$$

We integrate the system of equations from recombination at $z_{\text{rec}} = 1090$ to $z = 0$, where we specify our initial conditions by setting $h_i = 0.674$, where H_0 is $100 \frac{\text{km}}{\text{secMpc}} h_i$ in units of sec^{-1} . The radiation Ω_r and matter Ω_m components are dictated by the equations below [60, 61], where Ω_Λ follows from flatness:

$$\Omega_r = 4.15 \times 10^{-5} / h_i^2 \quad (8)$$

$$\Omega_m = 0.14241/h_i^2. \quad (9)$$

The densities are then determined by the following equations, where $\rho_{m,i}$, $\rho_{r,i}$, and $\rho_{\Lambda,i}$ are the total matter, radiation, and dark energy densities at recombination ($z = 1090$), respectively.

$$\rho_{\text{crit},0} = 3H_0^2/8\pi G \quad (10)$$

$$\Omega_\Lambda = 1.0 - \Omega_m - \Omega_r \quad (11)$$

$$\rho_{m,i} = \Omega_m \rho_{\text{crit},0} (1 + z_{\text{rec}})^3 \quad (12)$$

$$\rho_{r,i} = \Omega_r \rho_{\text{crit},0} (1 + z_{\text{rec}})^4 \quad (13)$$

$$\rho_{\Lambda,i} = \Omega_\Lambda \rho_{\text{crit},0} \quad (14)$$

B. Dynamical Dark Energy

We use the equation below to calculate $H(z)$ for a Universe with cold dark matter and dynamical dark energy [62]. We plot $H(z)$ from our model alongside $w_0 w_a \text{CDM}$, which has the equation of state parameter $w_{\text{DE}}(a) = w_0 + w_a(1 - a)$ for dark energy, to show that our model could display qualitative consistency with the DESI DR2 trends. In a following work, we plan to replace the cosmological constant with a quintessence field ($w > -1$) that is not coupled to the dark matter. This is appealing for avoiding the formation of a cosmological horizon, though it moves beyond a realization of Chen and Loeb's ideas, so we leave it to a separate paper. Similar to Chen and Loeb [19], who deferred a fit to DESI data to a separate study [20], we leave a full parameter fit to DESI results for future work. Such a fit is beyond the scope of the current study to explore the space of potentially viable models.

$$H(z) = H_0 \sqrt{\Delta}, \quad (15)$$

where

$$\Delta = \Omega_m (1+z)^3 + \Omega_r (1+z)^4 + \Omega_\Lambda (1+z)^{3(1+w_0+w_a)} \exp\left[-\frac{3w_a z}{1+z}\right]. \quad (16)$$

IV. RESULTS AND DISCUSSION

A. Effect on $H(z)$

In Figure 2 we plot $\Delta H/H$, the fractional change in the Hubble parameter, compared to standard ΛCDM . Our model produces qualitative similarity to the DESI observations as well as the $H(z)$ produced by Chen and Loeb with step-like changes in w . In the figure below, $\Omega_{\text{tot}} \approx 1$ at $z = 0$, which is not in tension with observational constraints on curvature [61].

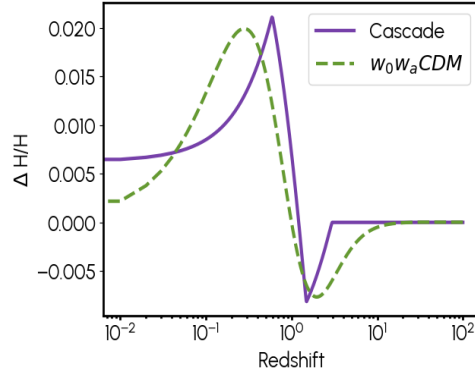


FIG. 2. The fractional change in $H(z)$ with our cascade compared to ΛCDM (solid). We also include a curve corresponding to dynamical dark energy with $w_0 = -0.83$ and $w_a = -0.62$, which produce behavior similar to that favored by DESI (dashed).

B. SIDM Cross Section

We show the momentum-transfer cross section as a function of velocity in Figure 3, with $m_\alpha = 1$ GeV, $m_h = 1$ MeV, and $g = 0.0175$. Note that m_α is the mass of the vector, m_h is the mass of the scalar mediator, and g is the effective coupling constant. We also plot the differential cross section in Figure 4 and Figure 5. It is clear that the cross section decreases with increasing relative velocity. Since $(g^2/4\pi)(m_\alpha/m_h) \approx 0.024 \ll 1$, perturbation theory is an appropriate approximation. Below we define the momentum-transfer cross section, σ_T [50]. This is more useful for SIDM than the total cross section, as it down-weights forward and backward scattering by including $(1 - |\cos(\theta)|)$ in the integral. We use θ for the scattering angle, Ω for the solid angle, M for the matrix element, and E_{cm} for the energy in the center-of-mass frame.

$$\sigma_T = 2 \int d\Omega (1 - |\cos(\theta)|) \frac{|M|^2}{64\pi^2 E_{\text{cm}}^2} \quad (17)$$

We include the closed-form expression for $|M|^2$ in the Appendix. We employ the tree-level cross section instead of partial wave analysis or the simpler Born approximation because the tree-level cross section captures physics that the other two do not. While partial wave analysis has been used to capture non-perturbative effects for a Yukawa interaction [63], we have vectors interacting via a scalar, rather than fermions. Massive vector fields differ from fermions because unlike fermions, they are bosons with three distinct polarizations, which affects the cross section. The Born approximation offers a simpler method for computing a cross section from a Yukawa potential, though it neglects the u -channel diagram, as well as the interference between t and u -channels [64], which our calculation incorporates. (See Figure 1 for a depiction of the t and u -channel processes.) One can view neglecting the u -channel as a simplifying approximation, though it dramatically changes $d\sigma/d\Omega$. A process that includes only the t -channel yields a differential cross section that peaks at $\theta = 0$ but not $\theta = \pi$, whereas the true differential cross section peaks at both $\theta = 0$ and $\theta = \pi$, producing a U-shaped

plot. This can in turn yield a noticeable impact on the momentum transfer cross section [64], so it is preferable to use the full tree-level cross section, when possible, even though this is more complicated to compute.

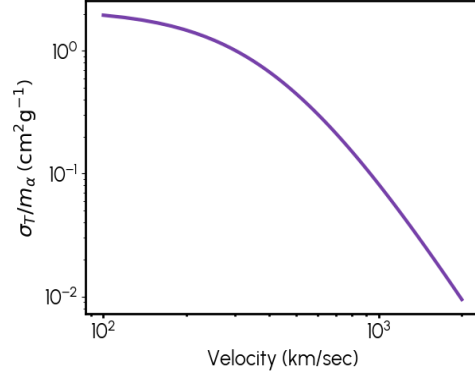


FIG. 3. We plot the tree-level momentum-transfer cross section for the scattering process $\alpha\alpha \rightarrow \alpha\alpha$ with $m_\alpha = 1$ GeV and $m_h = 1$ MeV. One can see that this decreases with increasing relative velocity, potentially enabling the SIDM to evade constraints from galaxy clusters while still producing cored density profiles in galaxies.

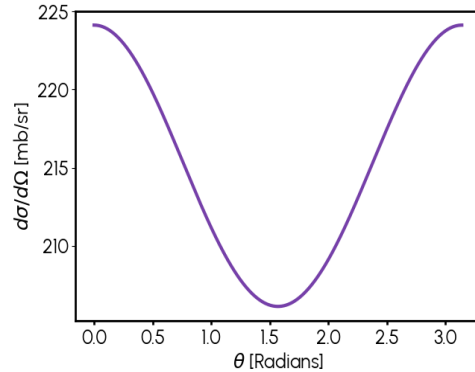


FIG. 4. We plot the tree-level differential cross section for the scattering process $\alpha\alpha \rightarrow \alpha\alpha$ with $m_\alpha = 1$ GeV, $m_h = 1$ MeV, and a relative velocity of 200 km/sec. This velocity is relevant for the Milky Way scale.

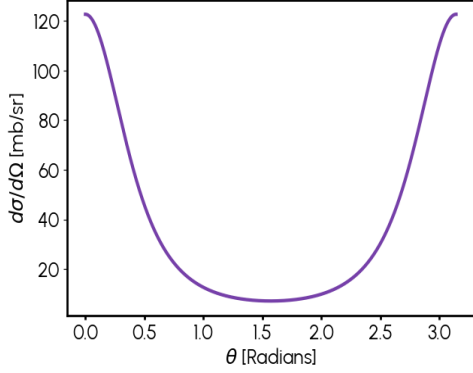


FIG. 5. We plot the tree-level differential cross section for the scattering process $\alpha\alpha \rightarrow \alpha\alpha$ with $m_\alpha = 1$ GeV, $m_h = 1$ MeV, and a relative velocity of 1000 km/sec. This velocity is relevant for the cluster scale. One can see that this cross section is suppressed as compared to the result for 200 km/sec.

V. CONCLUSION

We find it to be very difficult to produce a natural, fully renormalizable model that can realize the behavior desired by Chen and Loeb, though we are able to produce a more natural effective field theory that can generate similar behavior. This model also naturally yields a possible SIDM candidate as a consequence of gauge invariance. In a following work, we plan to replace the cosmological constant with a quintessence field not coupled to the dark matter. Future work could also fit the model parameters to DESI data, study effects on large-scale structure, consider production mechanisms for the dark matter, and more thoroughly investigate the SIDM candidate. It would be interesting to incorporate the tree-level differen-

tial cross section into N-body codes to correctly incorporate scattering that is both velocity-dependent, and anisotropic. While there are a few possibilities for production, one mechanism could involve inflaton decay [65], or coupling a dark vector field to the inflaton [66].

We emphasize that even if future work finds our fiducial model to be disfavored, this study is still valuable for studying the space of effective field theories that have the potential to realize the behavior desired by Chen and Loeb, which is relevant for finding a pathway towards explaining the DESI trends.

VI. ACKNOWLEDGEMENTS

KHB acknowledges the support of NSF 2125764.

VII. APPENDIX

A. S-Matrix Amplitude for Tree-Level Scattering Cross Section

Here we include a closed-form expression for the S-matrix amplitude used in plotting the SIDM cross section. This was produced from the t and u -channel Feynman diagrams via a manual computation. For compactness, we define C_1 , C_2 , and C_3 as the following quantities. We use p for the momentum, E_{cm} for the energy in the center-of-mass frame, θ for the scattering angle, m_h for the mass of the scalar mediator, and m_α for the mass of the vector field.

$$C_1 = \frac{1}{4}E_{\text{cm}}^2 - p^2 \cos \theta \quad (18)$$

$$C_2 = \frac{1}{4}E_{\text{cm}}^2 + p^2 \cos \theta \quad (19)$$

$$C_3 = \frac{1}{4}E_{\text{cm}}^2 + p^2 \quad (20)$$

$$|M|^2 = \frac{8g^4}{9m_\alpha^8} \left[\frac{4m_\alpha^4(C_1^2 + C_2^2 + C_3^2) + 2C_1^2C_2^2 - 8C_1C_2C_3m_\alpha^2}{(m_h^2 + 2p^2)^2 - 4p^4 \cos^2 \theta} + \frac{(C_1^2 + 2m_\alpha^4)^2}{(m_h^2 - 2p^2 \cos \theta + 2p^2)^2} + \frac{(C_2^2 + 2m_\alpha^4)^2}{(m_h^2 + 2p^2 \cos \theta + 2p^2)^2} \right] \quad (21)$$

B. Tree-Level Decay Rate

After symmetry breaking, we get interaction terms of the form $\frac{g_{AB}\nu}{\sqrt{2}}AB^\dagger B$, where ν is the VEV (vacuum expectation value) of the dark Higgs. The decay rate for $A \rightarrow B^\dagger B$ can be computed from the particle masses, m_A and m_B , and the coupling constant, g_{AB} , as shown below, with $c = 1$, ν in units of eV, masses in units of eV, $\hbar \approx 6.58 \times 10^{-16}$ eV · sec, and Γ in units of sec^{-1} . The mass of A (and by extension, the masses of B, C, and D) depends in part on the production mechanism for the dark matter. Future work can determine masses through a fit to observations after consideration of production mechanisms.

$$\Gamma_{A \rightarrow 2B} = \frac{g_{AB}^2 \nu^2}{16\pi \hbar m_A} \sqrt{1 - \frac{4m_B^2}{m_A^2}} \quad (22)$$

In our analysis, we neglect any energy transfer from A to h via $\frac{g_{AB}h}{\sqrt{2}}AB^\dagger B$, where h is the massive radial mode of the dark Higgs after

symmetry breaking. A more detailed analysis could consider this for the decay of A, as well as similarly for decays of B and C.

C. Clumping of Scalar Dark Matter

While the kinetic terms for a scalar field could suggest a sound speed of c , which might lead one to think that the particles would not clump, this is really only true when the particles are relativistic. The dark matter can still clump when particles are non-relativistic, if the dynamical time for gravity is less than the time required for particles to escape from an overdense region, as particles collapse under gravity before they are able to escape. The dynamical time is inversely proportional to the Hubble parameter, whereas the escape time is proportional to the particle mass, so when the mass is sufficiently large, the scalar field clumps like cold dark matter, rather than being a uniform field. This is in line with a large body of literature that considers scalar-field dark matter, whose mass is much larger than that of a quintessence field [67–72].

-
- [1] A. G. Riess *et al.*, Observational evidence from supernovae for an accelerating universe and a cosmological constant, *The Astronomical Journal* **116**, 1009 (1998).
 - [2] S. Perlmutter *et al.*, Measurements of Ω and Λ from 42 high-redshift supernovae, *The Astrophysical Journal* **517**, 565 (1999).
 - [3] P. J. E. Peebles and B. Ratra, Cosmology with a time variable cosmological constant, *Astrophysical Journal Letters* **325**, L17 (1988).
 - [4] B. Ratra and P. J. E. Peebles, Cosmological consequences of a rolling homogeneous scalar field, *Phys. Rev. D* **37**, 3406 (1988).
 - [5] I. Zlatev, L. Wang, and P. J. Steinhardt, Quintessence, cosmic coincidence, and the cosmological constant, *Phys. Rev. Lett.* **82**, 896 (1999).
 - [6] R. R. Caldwell, R. Dave, and P. J. Steinhardt, Cosmological imprint of an energy component with general equation of state, *Phys. Rev. Lett.* **80**, 1582 (1998).
 - [7] M. Abdul Karim *et al.* (DESI Collaboration), Desi dr2 results. i. baryon acoustic oscillations from the lyman alpha forest, *Phys. Rev. D* **112**, 083514 (2025).
 - [8] M. Abdul Karim *et al.* (DESI Collaboration), Desi dr2 results. ii. measurements of baryon acoustic oscillations and cosmological constraints, *Phys. Rev. D* **112**, 083515 (2025).
 - [9] K. Lodha *et al.*, Extended dark energy analysis using desi dr2 bao measurements, *arXiv e-prints*, arXiv:2503.14743 (2025), arXiv:2503.14743 [astro-ph.CO].
 - [10] T.-N. Li, P.-J. Wu, G.-H. Du, Y.-H. Yao, J.-F. Zhang, and X. Zhang, Exploring non-cold dark matter in the scenario of dynamical dark energy with desi dr2 data, *Physics of the Dark Universe* **50**, 102068 (2025).
 - [11] J. Khoury, M.-X. Lin, and M. Trodden, Apparent $w < -1$ and a lower s_8 from dark axion and dark baryons interactions (2025), arXiv:2503.16415 [astro-ph.CO].

- [12] M. Abedin, L. A. Escamilla, S. Pan, E. D. Valentino, and W. Yang, When dark matter heats up: A model-independent search for non-cold behavior (2025).
- [13] U. Kumar, A. Ajith, and A. Verma, Evidence for non-cold dark matter from desi dr2 measurements (2025), [arXiv:2504.14419 \[astro-ph.CO\]](#).
- [14] D. Wang, Evidence for dynamical dark matter (2025), [arXiv:2504.21481 \[astro-ph.CO\]](#).
- [15] W. Yang, S. Pan, E. Di Valentino, O. Mena, D. F. Mota, and S. Chakraborty, Probing the cold nature of dark matter, *Phys. Rev. D* **111**, 103509 (2025).
- [16] Y.-H. Yao, Y.-H. Shen, T.-N. Li, G.-H. Du, and Y. Gong, Examining a new form of non-standard dark matter using desi dr2 data (2025), [arXiv:2510.13436 \[astro-ph.CO\]](#).
- [17] M. Scherer, M. A. Sabogal, R. C. Nunes, and A. De Felice, Challenging the Λ CDM model: 5σ evidence for a dynamical dark energy late-time transition, *Phys. Rev. D* **112**, 043513 (2025).
- [18] M. P. Dabrowski, Phantom dark energy and its cosmological consequences, in *The Eleventh Marcel Grossmann Meeting* (World Scientific Publishing, 2008) pp. 1761–1763.
- [19] X. Chen and A. Loeb, Evolving dark energy or dark matter with an evolving equation-of-state?, *Journal of Cosmology and Astroparticle Physics* **2025** (07), 059.
- [20] M. Braglia, X. Chen, and A. Loeb, Exotic dark matter and the DESI anomaly (2025), [arXiv:2507.13925 \[astro-ph.CO\]](#).
- [21] D. N. Spergel and P. J. Steinhardt, Observational evidence for self-interacting cold dark matter, *Phys. Rev. Lett.* **84**, 3760 (2000).
- [22] A. Kamada, M. Kaplinghat, A. B. Pace, and H.-B. Yu, Self-interacting dark matter can explain diverse galactic rotation curves, *Phys. Rev. Lett.* **119**, 111102 (2017).
- [23] T. Ren, A. Kwa, M. Kaplinghat, and H.-B. Yu, Reconciling the diversity and uniformity of galactic rotation curves with self-interacting dark matter, *Phys. Rev. X* **9**, 031020 (2019).
- [24] J. F. Navarro, C. S. Frenk, and S. D. M. White, The structure of cold dark matter halos, *The Astrophysical Journal* **462**, 563 (1996).
- [25] J. F. Navarro, C. S. Frenk, and S. D. M. White, A universal density profile from hierarchical clustering, *The Astrophysical Journal* **490**, 493 (1997).
- [26] A. D. Ludlow *et al.*, The mass profile and accretion history of cold dark matter haloes, *Monthly Notices of the Royal Astronomical Society* **432**, 1103 (2013), [https://academic.oup.com/mnras/article-pdf/432/2/1103/18454450/stt526.pdf](#).
- [27] G. Gentile, P. Salucci, U. Klein, D. Vergani, and P. Kalberla, The cored distribution of dark matter in spiral galaxies, *Monthly Notices of the Royal Astronomical Society* **351**, 903 (2004), [https://academic.oup.com/mnras/article-pdf/351/3/903/3595222/351-3-903.pdf](#).
- [28] K. A. Oman *et al.*, The unexpected diversity of dwarf galaxy rotation curves, *Monthly Notices of the Royal Astronomical Society* **452**, 3650 (2015), [https://academic.oup.com/mnras/article-pdf/452/4/3650/18237239/stv1504.pdf](#).
- [29] I. M. Santos-Santos *et al.*, Nihao – xiv. reproducing the observed diversity of dwarf galaxy rotation curve shapes in Λ CDM, *Monthly Notices of the Royal Astronomical Society* **473**, 4392 (2017), [https://academic.oup.com/mnras/article-pdf/473/4/4392/21878619/stx2660.pdf](#).
- [30] I. M. E. Santos-Santos *et al.*, Baryonic clues to the puzzling diversity of dwarf galaxy rotation curves, *Monthly Notices of the Royal Astronomical Society* **495**, 58 (2020), [https://academic.oup.com/mnras/article-pdf/495/1/58/33216644/staa1072.pdf](#).
- [31] J. F. Navarro, V. R. Eke, and C. S. Frenk, The cores of dwarf galaxy haloes, *Monthly Notices of the Royal Astronomical Society* **283**, L72 (1996), [https://academic.oup.com/mnras/article-pdf/283/3/L72/3305901/283-3-L72.pdf](#).
- [32] J. I. Read and G. Gilmore, Mass loss from dwarf spheroidal galaxies: the origins of shallow dark matter cores and exponential surface brightness profiles, *Monthly Notices of the Royal Astronomical Society* **356**, 107 (2005), [https://academic.oup.com/mnras/article-pdf/356/1/107/3575199/356-1-107.pdf](#).
- [33] A. Pontzen and F. Governato, How supernova feedback turns dark matter cusps into cores, *Monthly Notices of the Royal Astronomical Society* **421**, 3464 (2012), [https://academic.oup.com/mnras/article-pdf/421/4/3464/3832707/mnras0421-3464.pdf](#).

- [34] F. Governato *et al.*, Cuspy no more: how outflows affect the central dark matter and baryon distribution in Λ cold dark matter galaxies, *Monthly Notices of the Royal Astronomical Society* **422**, 1231 (2012), <https://academic.oup.com/mnras/article-pdf/422/2/1231/3466602/mnras0422-1231.pdf>.
- [35] R. Teyssier, A. Pontzen, Y. Dubois, and J. I. Read, Cusp-core transformations in dwarf galaxies: observational predictions, *Monthly Notices of the Royal Astronomical Society* **429**, 3068 (2013), <https://academic.oup.com/mnras/article-pdf/429/4/3068/3296859/sts563.pdf>.
- [36] A. Di Cintio *et al.*, The dependence of dark matter profiles on the stellar-to-halo mass ratio: a prediction for cusps versus cores, *Monthly Notices of the Royal Astronomical Society* **437**, 415 (2013), <https://academic.oup.com/mnras/article-pdf/437/1/415/18452732/stt1891.pdf>.
- [37] J. Oñorbe, M. Boylan-Kolchin, J. S. Bullock, P. F. Hopkins, D. Kereš, C.-A. Faucher-Giguère, E. Quataert, and N. Murray, Forged in fire: cusps, cores and baryons in low-mass dwarf galaxies, *Monthly Notices of the Royal Astronomical Society* **454**, 2092 (2015), <https://academic.oup.com/mnras/article-pdf/454/2/2092/9503920/stv2072.pdf>.
- [38] T. K. Chan *et al.*, The impact of baryonic physics on the structure of dark matter haloes: the view from the fire cosmological simulations, *Monthly Notices of the Royal Astronomical Society* **454**, 2981 (2015), <https://academic.oup.com/mnras/article-pdf/454/3/2981/4038253/stv2165.pdf>.
- [39] E. Tollet *et al.*, Nihao – iv: core creation and destruction in dark matter density profiles across cosmic time, *Monthly Notices of the Royal Astronomical Society* **456**, 3542 (2016), <https://academic.oup.com/mnras/article-pdf/456/4/3542/9380435/stv2856.pdf>.
- [40] J. I. Read, O. Agertz, and M. L. M. Collins, Dark matter cores all the way down, *Monthly Notices of the Royal Astronomical Society* **459**, 2573 (2016), <https://academic.oup.com/mnras/article-pdf/459/3/2573/8105757/stw713.pdf>.
- [41] A. A. Dutton *et al.*, Nihao xx: the impact of the star formation threshold on the cusp-core transformation of cold dark matter haloes, *Monthly Notices of the Royal Astronomical Society* **486**, 655 (2019), <https://academic.oup.com/mnras/article-pdf/486/1/655/28320149/stz889.pdf>.
- [42] A. Benítez-Llambay, C. S. Frenk, A. D. Ludlow, and J. F. Navarro, Baryon-induced dark matter cores in the eagle simulations, *Monthly Notices of the Royal Astronomical Society* **488**, 2387 (2019), <https://academic.oup.com/mnras/article-pdf/488/2/2387/28979701/stz1890.pdf>.
- [43] A. Lazar *et al.*, A dark matter profile to model diverse feedback-induced core sizes of Λ CDM haloes, *Monthly Notices of the Royal Astronomical Society* **497**, 2393 (2020), <https://academic.oup.com/mnras/article-pdf/497/2/2393/33571817/staa2101.pdf>.
- [44] E. D. Jahn *et al.*, Real and counterfeit cores: how feedback expands haloes and disrupts tracers of inner gravitational potential in dwarf galaxies, *Monthly Notices of the Royal Astronomical Society* **520**, 461 (2023), <https://academic.oup.com/mnras/article-pdf/520/1/461/49003404/stad109.pdf>.
- [45] B. Azartash-Namin *et al.*, Bursting with feedback: The relationship between feedback model and bursty star formation histories in dwarf galaxies, *The Astrophysical Journal* **970**, 40 (2024).
- [46] J. Sánchez Almeida, I. Trujillo, and A. R. Platinio, The stellar distribution in ultrafaint dwarf galaxies suggests deviations from the collisionless cold dark matter paradigm, *The Astrophysical Journal Letters* **973**, L15 (2024).
- [47] M. Duch, B. Grzadkowski, and D. Huang, Strongly self-interacting vector dark matter via freeze-in, *Journal of High Energy Physics* **2018**, 10.1007/JHEP01(2018)020 (2018).
- [48] L. Sagunski, S. Gad-Nasr, B. Colquhoun, A. Robertson, and S. Tulin, Velocity-dependent self-interacting dark matter from groups and clusters of galaxies, *Journal of Cosmology and Astroparticle Physics* **2021** (01), 024.
- [49] C. A. Correa, Constraining velocity-dependent self-interacting dark matter with the milky way’s dwarf spheroidal galaxies, *Monthly Notices of the Royal Astronomical Society* **503**, 920 (2021), <https://academic.oup.com/mnras/article-pdf/503/1/920/36616545/stab506.pdf>.
- [50] C. A. Correa *et al.*, TangoSIDM: tantalizing models of self-interacting dark matter, *Monthly Notices of the Royal*

- Astronomical Society **517**, 3045 (2022), <https://academic.oup.com/mnras/article-pdf/517/2/3045/46586341/stac2830.pdf>.
- [51] K. R. Dienes and B. Thomas, Dynamical dark matter. i. theoretical overview, *Phys. Rev. D* **85**, 083523 (2012).
 - [52] K. R. Dienes and B. Thomas, Dynamical dark matter. ii. an explicit model, *Phys. Rev. D* **85**, 083524 (2012).
 - [53] K. R. Dienes and B. Thomas, Dynamical dark matter: Introduction, equation of state, and cosmological implications, *Proceedings of Science ICHEP2012*, 452 (2013).
 - [54] D. Harlow and H. Ooguri, Constraints on symmetries from holography, *Phys. Rev. Lett.* **122**, 191601 (2019).
 - [55] E. Witten, Symmetry and emergence, *Nature Physics* **14**, 10.1038/nphys4348 (2018).
 - [56] D. Harlow and E. Shaghoulian, Global symmetry, euclidean gravity, and the black hole information problem, *Journal of High Energy Physics* **2021**, 10.1007/JHEP04(2021)175 (2021).
 - [57] M. Cvetič, D. Klevers, H. Piragua, and P. Song, Elliptic fibrations with rank three Mordell-Weil group: F-theory with $U(1) \times U(1) \times U(1)$ gauge symmetry, *Journal of High Energy Physics* **2014**, 10.1007/JHEP03(2014)021 (2014).
 - [58] F. Feruglio, A note on gauge anomaly cancellation in effective field theories, *Journal of High Energy Physics* **2021**, 10.1007/JHEP03(2021)128 (2021).
 - [59] L. A. Boyle, R. R. Caldwell, and M. Kamionkowski, Spintessence! new models for dark matter and dark energy, *Physics Letters B* **545**, 17 (2002).
 - [60] S. Dodelson, *Modern cosmology* (Elsevier, 2003).
 - [61] N. Aghanim *et al.*, Planck 2018 results - vi. cosmological parameters, *Astronomy and Astrophysics* **641**, A6 (2020).
 - [62] E. V. Linder, Exploring the expansion history of the universe, *Phys. Rev. Lett.* **90**, 091301 (2003).
 - [63] S. Tulin, H.-B. Yu, and K. M. Zurek, Beyond collisionless dark matter: Particle physics dynamics for dark matter halo structure, *Phys. Rev. D* **87**, 115007 (2013).
 - [64] S. Girmohanta and R. Shrock, Cross section calculations in theories of self-interacting dark matter, *Phys. Rev. D* **106**, 063013 (2022).
 - [65] T. Moroi and W. Yin, Light dark matter from inflaton decay, *Journal of High Energy Physics* **2021**, 10.1007/JHEP03(2021)301 (2021).
 - [66] M. Bastero-Gil, J. Santiago, L. Ubalde, and R. Vega-Morales, Vector dark matter production at the end of inflation, *Journal of Cosmology and Astroparticle Physics* **2019** (04), 015.
 - [67] J. Preskill, M. B. Wise, and F. Wilczek, Cosmology of the invisible axion, *Physics Letters B* **120**, 127 (1983).
 - [68] Y. M. Cho and Y. Y. Keum, Dilatonic dark matter - a new paradigm, *Modern Physics Letters A* **13**, 109 (1998), <https://doi.org/10.1142/S0217732398000152>.
 - [69] W. Hu, R. Barkana, and A. Gruzinov, Fuzzy cold dark matter: The wave properties of ultralight particles, *Phys. Rev. Lett.* **85**, 1158 (2000).
 - [70] A. Bernal, J. Barranco, D. Alic, and C. Palenzuela, Galactic dark matter halo made of spin-zero bosons, *AIP Conference Proceedings* **1241**, 335 (2010).
 - [71] J. Magaña and T. Matos, A brief review of the scalar field dark matter model, *Journal of Physics: Conference Series* **378**, 012012 (2012).
 - [72] E. G. M. Ferreira, Ultra-light dark matter, *The Astronomy and Astrophysics Review* **29**, 10.1007/s00159-021-00135-6 (2021).